RECOGNIZING MEANDERS
TO RECONSTRUCT RIVER DYNAMICS OF THE GANGES

E. A. Addink *, M. G. Kleinhans

Faculty of Geosciences, Utrecht University, PO Box 80115, 3508 TC Utrecht, The Netherlands –
(e.addink, m.kleinhans)@geo.uu.nl

Commission VI, WG VI/4

ABSTRACT:

The long-term discharge evolution of branches of rivers can potentially be derived from inactive and fossil river meanders using relations between discharge and channel width and meander dimensions. This evolution is relevant for the understanding of river dynamics and avulsion, and the resulting changes of downstream flooding risks and shipping conveyance. Unfortunately, digitalisation of infilled and overgrown meanders from images or maps is laborious and inaccurate.
We developed and demonstrated an automated procedure for the recognition of river meanders from satellite-imagery of the river Ganges. For this automated recognition we used object-based image analysis, which allows including shape and neighbourhood information besides spectral information in the classification procedure.
We needed information on both present, i.e. water carrying meanders, and fossil, i.e. partly vegetated meanders. This implies a wide range of spectral behaviour and hence the selection of meanders should be primarily based on shape. Therefore, we used an image showing the low-flow situation.
Results demonstrate that the object-oriented image analysis approach offers detailed meandering metrics. The Gorai channel belt, once the main courses of the Ganges, has a fairly uniform meander size distribution and only a small number of old meanders, indicating a sudden emergence of the channel with limited dynamic meandering and a short period of activity. The Hooghly channel belt, another previous main course, has many more abandoned meanders and cut-off meanders including many small ones, suggesting a more gradual rise of discharge and a longer period of activity. The lack of small meanders in the present residual channels indicates that both were abandoned so suddenly that meander geometry could not adjust to the waning discharge.
Given the importance of shape to recognize the meanders, this study was possible only thanks to the availability of object based image analysis.

1. INTRODUCTION

1.1 Ganges delta

The course of the Ganges river shifted to the east over the past centuries by avulsion: sudden shifts of the channel where a new course is found through former floodplains. The avulsions of the Ganges are attested by the presence of residual channels, by historical and geological records, e.g. the fact that the major historical harbour city, Calcutta, is located on a minor channel : the Hooghly river (cf. Coleman 1969).
The Ganges River emerges near the Tibet-India border and flows southeast across India into Bangladesh, and into the Bay of Bengal. Prior to the 16th century the Hooghly river conveyed most of the discharge of the Ganges. A later course is the Gorai river, which even today suffers from decreasing discharge and fairway depth because a disproportionally large amount of sand enters the Gorai at its offtake from the Ganges. At present the Ganges confluences with the Brahmaputra to form the Meghna river and the nearly abandoned channels of the Ganges are expected to silt up further.

1.2 River Morphometry

For prediction of future flooding risks and shipping fairway depth, understanding is required on the evolution of channels that are being abandoned in the avulsion process. The rate of evolution is largely controlled by the detailed dynamics of the river bifurcation (Kleinhans et al. in press), but this cannot be recovered accurately for historical cases. Instead, we study a proxy for the discharge in (nearly) abandoned channels: the geometry of meanders.
Empirically, the length of meanders is related to discharge. The underlying relation is that channel width is related to a representative discharge; bar pattern is related to the channel width/depth ratio and meander bend erosion is related to the bar pattern. The exact relations between discharge, width and meander geometry vary with discharge regime, the nature of the channel sediment and of the floodplains, but this requires much further study so at present the empirical relations must suffice for a semi-quantitative comparison between former courses of the same river. Furthermore, these empirical relations are supported by recent meander simulation modelling (Camporeale et al. 2005). We use the following approximate relations inversely to infer discharge from meander geometry statistics: $\lambda=10W$ and $W=10Q^{1/2}$ so that $\lambda=100Q^{1/2}$, where

---

* Corresponding author.

λ=meander wavelength, W=channel width and Q=flow discharge. In the process of meander formation and displacement, neck cutoffs take place so that meander bends are abandoned. By comparing older meander bends with bends in the present channel, the change of discharge over time can be inferred. Given that time is needed for a river to adjust meander wavelength to a changing discharge regime, the rate of change relative to the minimum time needed for adaptation can be inferred.

1.3 Channel metrics and remote sensing

Satellite images show river channels, both active and fossil, very well. Images taken at low discharge moments are superior to images recorded at high discharge moments.

Meanders may still be active and carry water, or they may have been abandoned and be in some revegetating state. Spectrally, they can show a wide range of values, thus limiting the viability of spectral analysis to delineate meanders. However, whatever land cover they might have, the shape of both active and fossil meanders is so characteristic that it is easily recognized in images by human eye.

Since meanders are to be recognized on their shape, object-based image analysis seems a promising method to delineate them in satellite imagery. Once they have been delineated, their metrics and spectral behaviour can be analysed.

For a larger project (in progress), we collected seven scenes from Landsat MSS and TM recorded in 1975, 1990 and 2000. By reconstructing the river dynamics for those years, we will gain insight in the discharge changes in the periods in between.

The aim of this paper is the proof of concept that meanders can be delineated in satellite imagery using segmentation techniques. We will demonstrate how the meanders can be extracted from satellite images for a subset of the delta.

Figure 1. Location of the study area outlined in black (source ESRI)

2. DATA AND METHODS

2.1 Study area

The area that we selected to develop the method is located in the western part of the Ganges delta. The largest part lies in West Bengal, India, while the eastern part extends into Bangladesh (figure 1). It measures 70*90 km^2. The landscape has been shaped by fluvial processes and is a patchwork of fossil meanders cross cut by active channels. The land cover stages of the fossil meanders range from open water to fully revegetated.

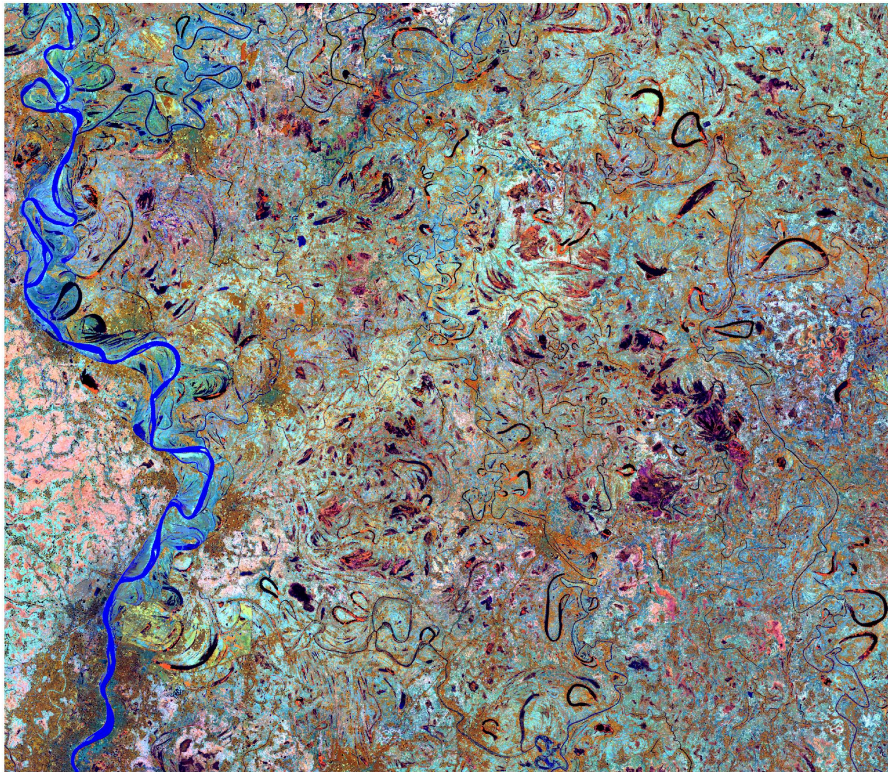Land use comprises mainly agricultural and some urban areas.

Figure 2. Landsat TM image, 14 November 1990. RGB 453

2.2 Data

For the area we selected a Landsat TM image recorded in November 1990 during the dry season (figure 2).

We excluded the thermal band from further use, because its relatively high temporal variability and its lower spatial resolution would reduce the applicability of the developed method to the larger area. The remaining six bands were all normalised to a mean value of 120 and a standard deviation of 20 in order to give them equal weight during the segmentation process.

2.3 Methods

We will develop an object-oriented classification method of satellite imagery. For comparison, we will perform a pixel-based classification.

Pixel-based classification

We classified the image using a clustering approach. Ten clusters were defined, two of which represented open water. One showed open water with a sediment load, i.e. active channels; the second cluster represented (parts of) fossil meanders still carrying water. The remaining eight clusters represented different terrestrial land cover classes.

Segmentation

The normalised Landsat TM images was segmented at different heterogeneity levels using eCognition version 3.1 (Definiens, 2003). The segmentation process is region based and allows to indicate a balance between spectral properties and shape characteristics, defined by smoothness and compactness (Benz et al., 2004). We set this balance such that spectral properties steered the process for 60% and shape properties for 40%. Shape properties were fully determined by smoothness and not

at all by compactness, since meanders tend to be smooth and elongated, i.e. not compact.

The maximum internal heterogeneity of the objects is set by the scale parameter, the effect of which is data-set specific (Addink et al., 2007). Since meanders of different sizes often show different internal spectral variation when recorded with a 30m pixel, we segmented the image several times with different values for the scale parameter: 5, 7, 10, 15 and 20. Visual interpretation learned that larger values would often result in objects including a fossil, vegetated, meander and part of the surrounding vegetated area.

Distinguishing meanders

Visual interpretation clearly allows for detection of meanders in the image. However, the aim of this project is to automate this. Therefore training sets were created by selecting 30 meanders by hand in each of the different object sets. Besides, 30 non-meander objects were selected randomly. I.e., all objects got assigned a random number and the first 30 that did not have the shape of a meander were selected. During these selection processes only the outlines of the objects were visible, no spectral information was displayed.

For the training sets a set of four variables describing the object shape was created: *length/width*, *shape index*, *curvature*, *length/width of skeleton.Length/width* divides the longer side of the bounding box by the shorter side. *Shape index s* is defined by

$$s = \frac{e}{4\sqrt{A}}$$

where e is the border length of the object and A the object area. *Curvature* is based on the skeleton of an object and is an indicator for the change in direction within an object; and *length/width of skeleton* is the length of the backbone of an object divided by the largest distance perpendicular to it.
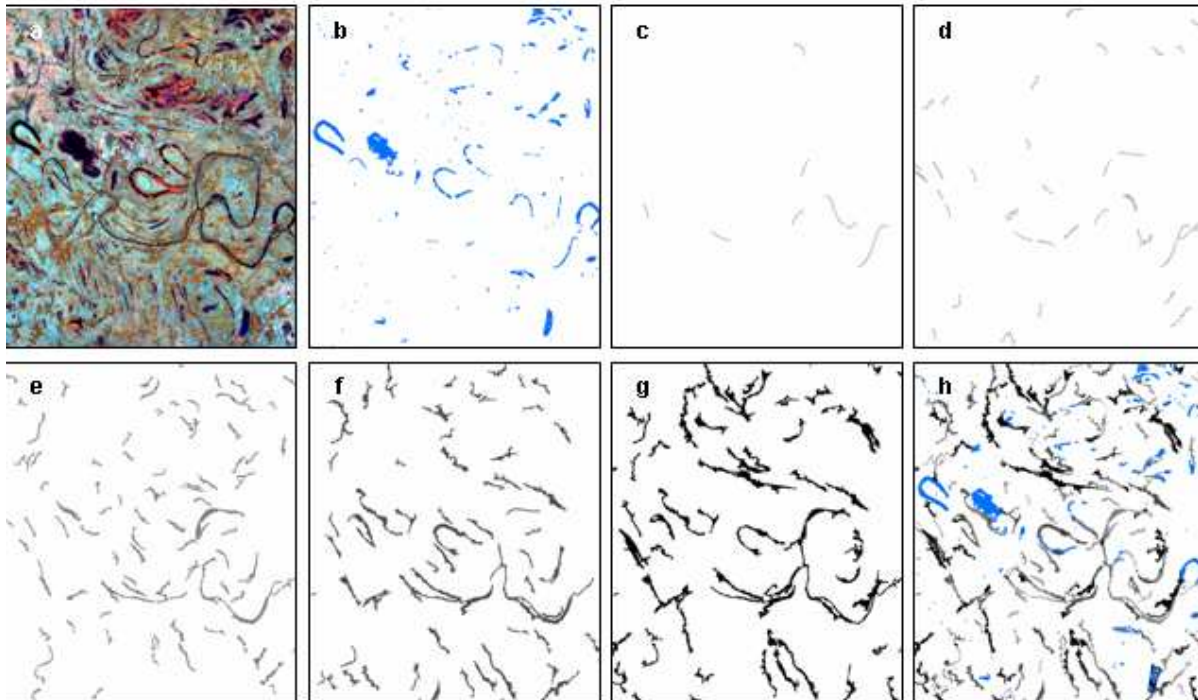

Figure 3. Example of channel identification for a sample area. A shows the original image, b shows the pixel-based water classification, c –g show the channel objects derived from segmentations with scale parameters 5, 7, 10, 15 and 20 respectively, h shows the combination of object and pixel information
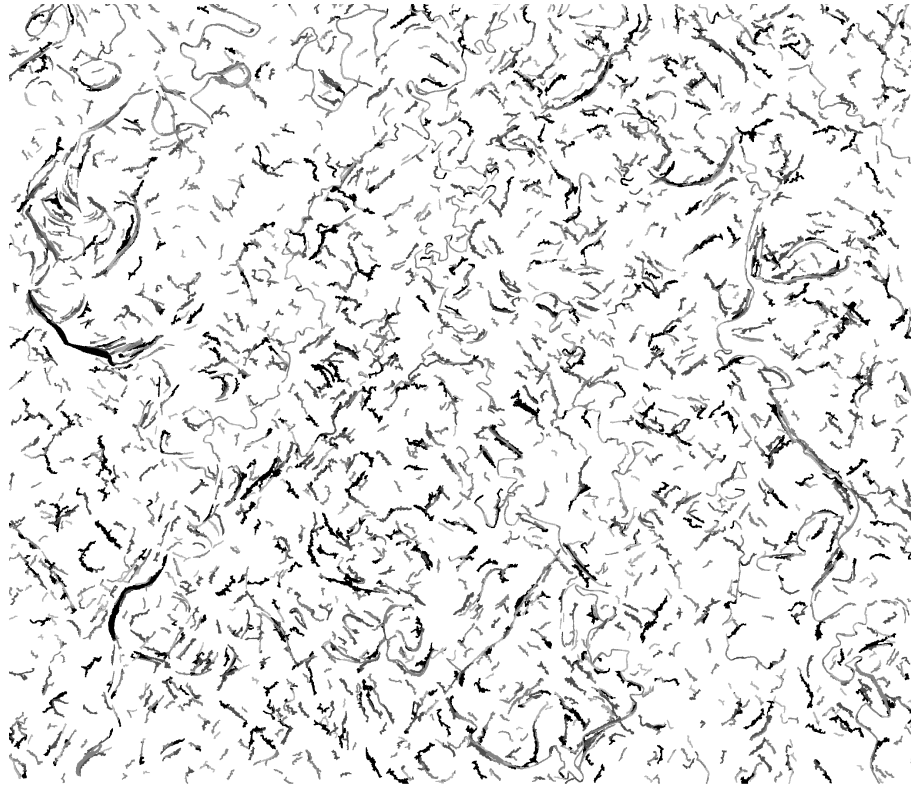
Figure 4. Object-based channels. Colors follow the color scheme as in figure 3.
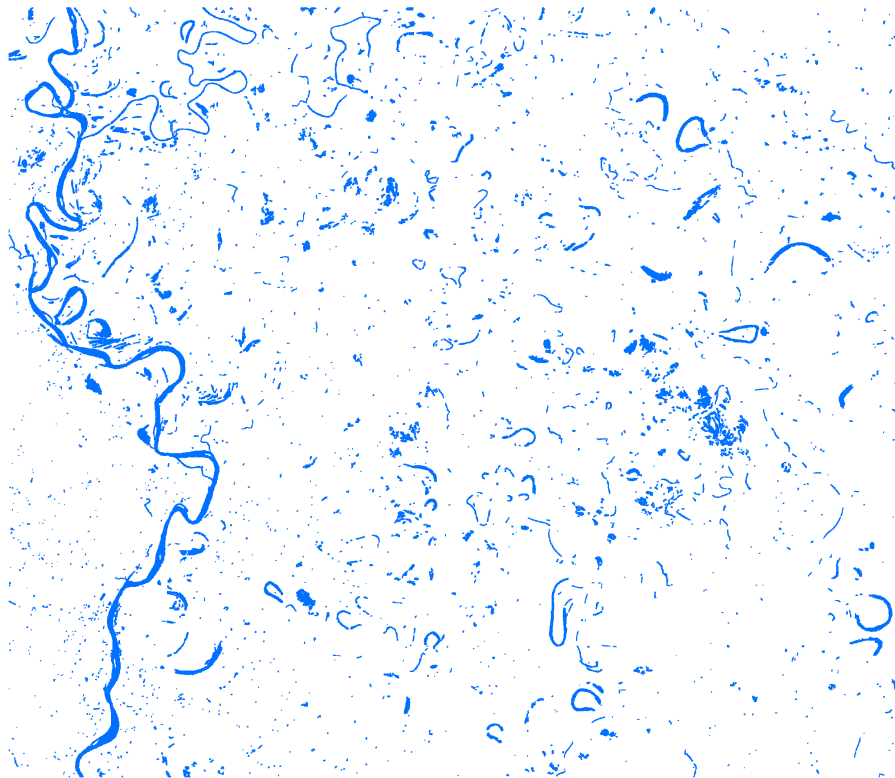

Figure 5. Pixel-based map of water

Classification trees were applied to each training set and to all sets combined classification trees. Classification trees are fitted by recursively partitioning the data set into smaller subdivisions on the basis of rules on the independent variables that optimize the classification, i.e., the dependent variable (Breiman et al., 1984). Because each partitioning is made on the basis of the independent variable that produces the most homogeneous subsets of the classes at each step (measured using deviance), the fitting algorithm results in the optimal distinction between classes and yields an explicit and intuitive understanding of relationships (in the form of a decision tree) between the dependent variable (i.e., channel or non-channel) and the independent variables (Friedl and Brodley, 1997). This provides good insight into the steps taken to distinguish the classes (Hansen et al., 2000).

To define classification trees training sets are needed. Once they have been defined they can be applied to any data set that contains the relevant variables. All data entries in the set are led through the tree and get assigned the class of the respective end member.

Combining different scales

All object sets were classified using the classification trees. All objects that were recognized as a meander were selected. They were all merged into one layer, showing the meanders detected in the image by object-oriented analysis.

Integrating pixel-based classification with objects

To further improve the results, information from the pixel-based classification was combined with the object-based meanders. As became clear during the analysis, some parts of the meanders show too much internal contrast to be delineated as a single object. The comprising objects will not show the characteristic elongated, curved shape and will hence not be classified as meander. For all objects that belong to open water, we know that they are part of a meander, either active or fossil. Therefore we selected all objects that contained at least 85% water and classified them as channel.

3. RESULTS

The number of objects decreased exponentially with increasing values for the scale parameter: 442600 to 28600 with scale parameters of 5 and 20 respectively. Accordingly, the size of the objects increased with higher scale parameter values.

The classification trees revealed that the best variable to distinguish channel objects from non-channel objects was the shape index, and that adding more variables did not significantly improve the accuracy. For the different segmentation sets, the channel objects would be found in the higher range of the shape index values. The threshold to distinguish between the two categories increased slightly with increasing scale parameters; from 2.49 with scale parameter 5 to 3.3 with scale parameter 20. Accuracy values for the different trees ranged from 80 to 90%.

The object sets were subjected to the corresponding classification trees to label the channel objects. In figure 3 a sample area is shown with results from all scales. Obviously, some objects would remain unchanged over the different scales and would pop-up as a meander at different scales. The channel objects were combined into one layer to combine the channels created at different discharge levels and hence of different sizes (figure 4).
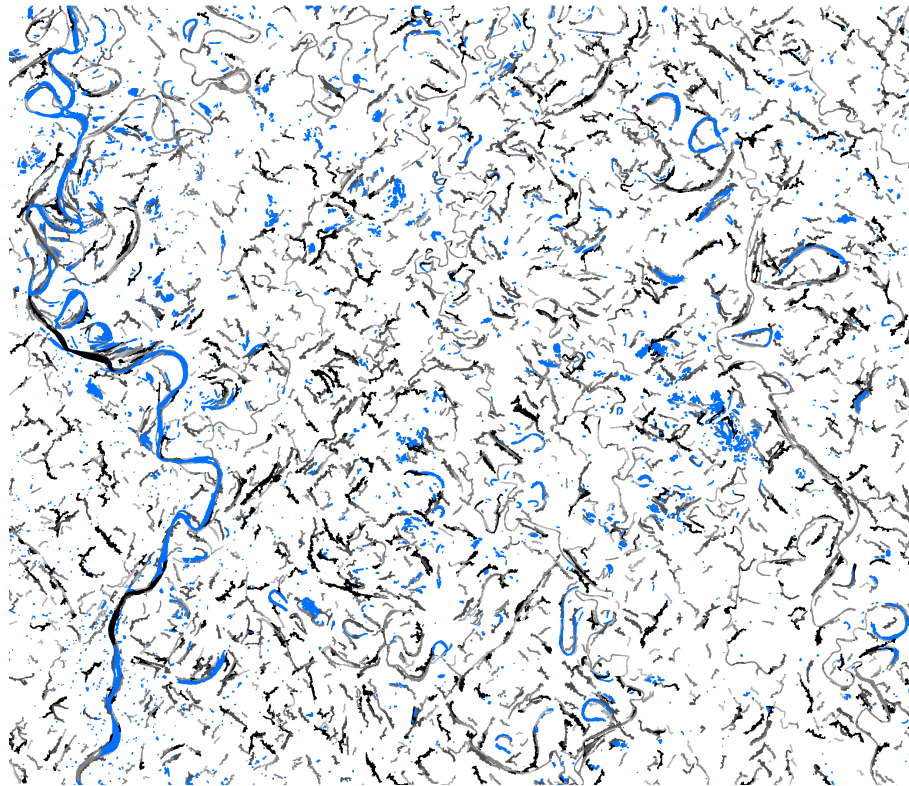

Figure 6. Object-based channels combined with water pixels. Color scheme follows figure 3.

Object sets resulting from the higher scale parameter values sometimes suffered from pollution by non-channel objects with an elongated shape.

The pixel-based classification clearly shows the channels that are currently still active (figure 5). Comparing figures 4 and 5 reveals that the object approach and the pixel approach partly yield the same results, but that particularly the larger channels are not detected by the object approach. The two approaches yield partly complementary information. As not to loose the information held in the pixel-based map, we decided to combine the two resulting maps (figure 6).

4. DISCUSSION AND CONCLUSIONS

The method presented here allows delineation of channels, both active and inactive. Besides, it allows characterization of their metrics, thus allowing the reconstruction of discharge volumes during their formation.

The object- and pixel-based maps currently provide complementary information. At higher scale parameters, the object-based channel maps are polluted by non-channel objects with an elongated shape. This was the major reason not to include higher scale parameter values in the analysis. This issue deserves further attention in order to delineate the larger channel objects as well. It is anticipated that by fine-tuning the threshold value, this pollution will be largely reduced and that the major channels then will be available from the object-approach.

Currently no methods are available to delineate channels that are not active anymore, from satellite imagery. The method presented here is capable of selecting both active and fossil channels. However, visual comparison of the channel map with the image reveals that not all channels are detected, yet. Even though object-based image analysis comes much closer to human vision than pixel-based image analysis, a gap remains between the two.

Refinements of the method in the near future will consist of exploring the additional value of including scale parameters smaller than 5. Furthermore, the pixel-based classification shows many small lakes, consisting of about 5 pixels with a round shape. These will be removed from the channel map.

In the somewhat further future we will look into the possibilities to reconstruct the historic fluvial dynamics of the Ganges delta using the channel map. Therefore, it would be very valuable if the relative age of meandering channels could be determined from the images as well, possibly based on vegetation development.

We conclude by stating that we developed an entirely new approach to image analysis for fluvial purposes. The method as we developed is well capable of delineating channel objects from a Landsat TM image. Some refinements are needed to include the large channel objects as well. At the moment this is well solved by combining the object channel map with the pixel water map.

REFERENCES
Addink, E.A., De Jong, S.M. and Pebesma, E.J., (2007). The importance of scale in object-based mapping of vegetation parameters with hyperspectral imagery. Photogrammetic Engineering & Remote Sensing, 73(8), pp. 905-912.

Benz, U.C., Hofmann, P., Willhauck, G., Lingenfelder, I. and Heynen, M., (2004). Multi-resolution, object-oriented fuzzy analysis of remote sensing data for GIS-ready information. ISPRS Journal of Photogrammetry and Remote Sensing, 58(3-4), pp. 239-258.

Breiman, L., Friedman, J.H., Olshen, R.A. and Stone, C.J., 1984. Classification and Regression Trees, 358pp. (Monterey, California: Wadsworth).

Camporeale, C., P. Perona, A. Porporato, and L. Ridolfi, (2005). On the long-term behavior of meandering rivers, Water Resour. Res., 41, W12403, doi:10.1029/2005WR004109.

Coleman, J.M., (1969). Brahmaputra River: channel processes and sedimentation, Sediment. Geol., 3, pp 129-239.

Definiens, 2003. eCognition user guide 3

Friedl, M.A. and Brodley, C.E., 1997. Decision tree classification of land cover from remotely sensed data. Remote Sensing of Environment, 61, pp. 399-409.

Hansen, M.C., Dubayah, R. and DeFries, R.S., 1996. Classification trees: an alternative to traditional land cover classifiers. International Journal of Remote Sensing, 17(5), pp. 1075-1081.

Kleinhans, M.G., H.R.A. Jagers, E. Mosselman, and C.J. Sloff (in press). Bifurcation dynamics and avulsion duration in meandering rivers by 1D and 3D models, Water Resour. Res.